Arch. Mech., 40, 5-6, pp. 581-594, Warszawa 1988

Numerical and experimental study of a form of damage in plasticity

T. DESOYER (POITIERS), O. DEBORDES (MARSEILLE)
and A. DRAGON (POITIERS)

THE DAMAGE mechanism by oriented cavity growth from hard inclusions in metals is examined from the viewpoint of mechanical factors conditioning its evolution. The basic features of the homogenization procedure applied by DRAGON [1] to set up damage evolution equations are confronted with experimental and numerical simulations. The experimental approach is only briefly referred to. Attention is particularly focused on the finite element investigation of the problem for a basic cell subjected to boundary conditions relevant to periodicity of the aggregate due to regular inclusion spacing. The contact finite elements are employed on the matrix-inclusion interface within the cell. The local matrix deformations are studied and correlated with the cavity growth after debonding. Numerical results in terms of the components of the hybrid damage tensor are given for some loading paths.

Celem pracy jest analiza mechanizmu uszkodzenia materiału przez zorientowany wzrost pustek wokół twardych wtrąceń w metalach z punktu widzenia czynników wpływających na ich ewolucję. Podstawowe cechy procedury homogenizacyjnej zastosowanej przez A. DRAGONA [1] do sformułowania równań ewolucji uszkodzeń porównano z symulacją eksperymentalną i numeryczną. Wyniki badań eksperymentalnych przedstawiono skrótowo. Główny nacisk położono na rozwiązywanie metodą elementów skończonych zadania dla podstawowej komórki z nałożonymi warunkami brzegowymi, związanymi z okresowością budowy agregatu spowodowaną regularną strukturą wtrąceń. Na powierzchni granicznej, matryca–wtrącenie, zastosowano skończone elementy kontaktowe. Zbadano lokalne deformacje matrycy i skorelowano je ze wzrostem pustek. Rezultaty numeryczne wyrażone w składowych hybrydowego tensora uszkodzenia przedstawiono dla różnych dróg obciążenia.

Целью работы является анализ механизма повреждения материала через ориентированный рост пустот вокруг твердых включений в металлах с точки зрения факторов влияющих на их эволюцию. Основные свойства гомогенизационной процедуры применены А. Драгоном [1] для формулировки уравнений эволюции повреждений и сравнены с экспериментальной и численной имитациями. Результаты экспериментальных исследований представлены сжатым образом. Главное внимание обращено на решение методом конечных элементов задачи для основной ячейки с наложенными граничными условиями, связанными с периодичностью строения агрегата, вызванной регулярной структурой включений. На граничной поверхности матрица–включение применены конечные контактные элементы. Исследованы локальные деформации матрицы и они коррелиированы с ростом пустот. Численные результаты, выраженные в составляющих гибридного тензора повреждения, представлены для разных путей нагружения.

1. Introductory remarks on homogenization. Scope of study

THE DAMAGE phenomenon is commonly qualified as "ductile" when it is coupled with more or less advanced plastic deformations. Focusing on the plastically deforming metals at ambient temperatures, the damage process is principally due to the nucleation and growth of voids around inclusions and second phase particles. Passing through void coalescence mechanisms, it leads eventually to failure relative to the development of a macroscopic crack, see, e.g. BEREMIN [2]. The complex stress/strain configurations

are inherent to the yielding pattern on the microscale where inclusion misfit and subsequent cavity growth occur.

In order to study and to quantify macroscopic consequences of such events, it is preferable to employ something more than just a single scale phenomenological viewpoint in the framework of damage- and plasticity-modelling with intuitively guided selection of thermodynamic state variables. Indeed, to distinguish and control eventually the principal factors influencing the overall properties and the evolution of a heterogeneous medium, it is useful to go down to the scale level well enough to discern relative heterogeneities. On such a level the characteristic size of constituents and heterogeneities (inclusions, cavities, microcracks) becomes of the order of a unity. In other words, by a proper rescaling one has an enlarged view of what is beforehand chosen as a representative volume element or a unit cell of a material. By determining local fields in the cell through the solution of a proper auxiliary "microscopic" boundary-value problem or having just effected useful estimations of the micro-constitutive laws and local fields, one may proceed to relate the corresponding macro-variables through the homogenization process, see SUQUET [3]. In such a way one may precise, for example, an overall elastic behaviour and also, under some conditions, the dissipative one, e.g. the plasticity and/or damage relationships for an aggregate. The accuracy of homogenization depends on the degree of refinement of the analysis of the micro-mechanisms concerned. The behaviour of an equivalent homogeneous medium the one viewed on a macroscale, is the one of the given heterogeneous "real" material, when the phenomena of interest are viewed "globally", i.e. on a very large scale with respect to that of the size of heterogeneities.

The homogenization approach largely exploited in continuum mechanics, e.g. in the context of polycrystalline aggregates is the one deriving from the Hill–Mandel mean-value or averaging method, see, for example HILL [4]. In general framework of analytical connection between the local deformation of individual constituents in situ and the overall behaviour of an aggregate (composite material), the employment of the averaging method gives rather rough estimations with regard to the convergence methods using asymptotic developments, SANCHEZ [5]. Nevertheless, it remains reasonable for the moderate concentrations of heterogeneities (up to $\sim 20\%$) with a representative volume element cautiously defined, i.e. sufficiently large, with no heterogeneities meeting its boundary. The framework wherein the choice of mean values as the limits of highly oscillating local fields relative to heterogeneities is justified in the sense of convergence is the one characterized by periodicity of the aggregate. In the latter context the relative homogenization is thus exact. In the sequel we postulate the quasi-periodicity for a matrix-with-inclusions aggregate in a reference configuration (no damage) resulting from a regular inclusion spacing. Consequently, for the damaged material (cavities around inclusions) the basic cell can be regarded as an element containing a single defect (oriented cavity partially or totally separated from an inclusion) surrounded by a ductile homogeneous matrix. The micro-defects (cavities) represent specific heterogeneities for the damaged medium. Their size can vary continuously on the macroscopic scale. However, viewed on the microscale (enlarged domain), these size variations as well as those of the variables involved in are not perceived. The material remains quasi-periodic in the presence of damage, SUQUET [3], CHIHAB and DRAGON [6].

For a basic cell located sufficiently far from the boundary of the homogeneous body,

the fields representing stress $\boldsymbol{\sigma}$, strain $\boldsymbol{\epsilon}$ and eventually other quantities, conform at the microscopic level to the periodicity of the geometry: they represent periodic fields. The local fields $\boldsymbol{\sigma}(z; x)$ and $\boldsymbol{\epsilon}(z; x)$ as depending on the "macroscopic" coordinates z $(z_i; i = 1, 2, 3)$ can vary from one place to another in a way similar to that of their averages $\bar{\boldsymbol{\sigma}}(z)$, $\bar{\boldsymbol{\epsilon}}(z)$. The local variations accounted for by their dependence on x are supposed to be periodic; $x|x_i$, $i = 1, 2, 3$, are the "microscopic" coordinates after rescaling. This leads to the formulation of the specific periodicity boundary conditions for the local boundary-value problem for the cell. These conditions reflect the periodic character of stress and strain at the microscopic scale and differ much from Hill's classical conditions postulating the uniformity of the stress or that of the strain on the cell faces. The periodicity boundary conditions are more akin to the weakened Hill's conditions (see HILL [4]) requiring the respective fields to be merely "macroscopically uniform" on the cell boundary (macro-homogeneity assumption). As regards the boundary conditions for the local problem in the ductile fracture context, see, for example GILORMINI *et al.* [7].

At the beginning (Sect. 2) the concept of damage-related tensorial variables is briefly resumed. Particular forms of these variables are made suitable to the homogenization context given above (periodicity, the basic cell containing a single cavity). The definition of a damage tensor supposes appropriate averaging over the basic cell which assures the macroscopic character of the entity in question while conserving the essential features of the micro-events relative to the damage mechanism as, for example, non-spherical cavity forms. Furthermore, a return to the micromechanics problem is operated. Its solution, i.e. determining microscopic fields for given global (mean) quantities, makes it possible to establish the damage evolution relationship by homogenization. It is stressed that the expression for the local velocity field in the matrix and in particular its form on the cavity surface constitutes the basis for the homogenization procedure mentioned. The latter allows to express the damage tensor rate $\dot{\boldsymbol{\varphi}}$ as a function of the global strain rate $\bar{\dot{\boldsymbol{\epsilon}}}$, of the actual damage $\boldsymbol{\varphi}$ and eventually of some scale and periodicity factor k.

The finite element approach for the basic cell problem is considered in Sect. 4, the cell domain being subjected to the periodicity boundary conditions. The latter allows in some manner to account for the effect of interaction between neighbouring cells (and cavities), see [7]. The experimental tests resumed in Sect. 3 were intended to follow the void growth from artificial inclusions periodically spaced. The tests and their finite element simulation for a whole specimen with a limited number of cells seem to confirm the periodicity of local fields and the choice of relative boundary conditions for the basic cell.

In the finite element analysis of the cell problem (Sect. 4) the matrix and inclusion materials are assumed as elastic-plastic with isotropic hardening in finite strain; the rigidity of an inclusion is taken to be much higher in comparison to that in a matrix. The singular interface finite elements completing the code MEF-Plasticity (origin: UTC-Compiegne, G. Touzot, modified into a large strain version by Debordes, see [8]) are employed on the matrix inclusion interface as long as the contact is assured. Several global histories are considered for the plane strain case. The displacement increment charts and those concerning the evolution of plastic deformations in the matrix are correlated with void-shape changes. The results of numerical homogenization regarding the damage kinetics in terms of damage tensor components are presented.

Concluding remarks (Sect. 5) concern diverse correlations, e.g. those between the macrostress-macrostrain curves and cavity growth, the effect of inclusion presence on plastic strain localization and the like subjects.

2. Damage tensors. Evolution of damage from the solution of a local problem

In the presence of damage zones as cavity-like microdefects the averaging in the basic cell is still well-founded if accounting for extended fields to the interior of a cavity. When the kinematic quantities like the deformation gradient $\mathbf{F}$, the displacement gradient $\nabla\mathbf{u}$, i.e. different strain tensors, are considered, the actual position vector $\mathbf{x}$ and the displacement $\mathbf{u}$ are respectively extended. The extended fields may be arbitrary except for verifying necessary regularity postulates and being compatible with the real matrix field at the cavity surface. So, only the surface expressions relative to cavity deformation are kinematically consistent, see, to example BUI *et al.* [9], DRAGON and CHIHAB [10] and also [3, 6]. For the displacement gradient the surface expression and its volumetric counterpart have the following classical form:

$$\int_{\partial v_c = s_c} (\mathbf{u}\otimes\mathbf{n})\,ds = \int_{v_c} \nabla\mathbf{u}\,dv, \tag{2.1}$$

with $\mathbf{n}$ standing for an outward unit normal to the current cavity surface s_c, and v_c representing the actual cavity domain. For the sake of simplicity v_c will also stand for the volume of v_c. A microcrack may be looked upon as a limiting case of a cavity. As the displacement discontinuity $\mathbf{b} = [\mathbf{u}]$ is to be considered across the surface s_c at a point of a normal $\mathbf{n}$, the displacement gradient in the cavity tends to infinity. It does it in a manner that its volume integral over the cavity remains finite, see, for example, HORII and NEMAT-NASER [11]. By introducing the delta functional $\delta(s_c)$ on the proper space of functions, we have analogously to Eq. (2.1)

$$\int_{\partial v_c = s_c} (\mathbf{b}\otimes\mathbf{n})\,ds = \int_{v_c} (\mathbf{b}\otimes\mathbf{n})\,\delta(s_c)\,dv. \tag{2.2}$$

In the case of a cavity and/or microcrack growing from the matrix inclusion interface, one can interpret $\mathbf{b}$ as the decohesion (debonding) displacement. Noting by ${}_c\mathbf{x}$ the current position of a material point on the cavity surface and by ${}_i\mathbf{X}$ its reference position coinciding with a point on the inclusion surface, i.e. the interface corresponding to initial (perfect) cohesion, we have (Fig. 1)

$${}_c\mathbf{x} = {}_i\mathbf{X} + \mathbf{b}, \qquad {}_c\dot{\mathbf{x}} = \dot{\mathbf{b}}, \tag{2.3}$$

where the dot stands for the time derivation. We may repeat the argument (2.1)–(2.2) for the velocity field replacing the displacement one. For a single cavity within the representative volume element (the basic cell), the averaging formulae for the rate of the deformation gradient (the Lagrangian velocity gradient) $\dot{\mathbf{F}}$, the Eulerian velocity gradient $\nabla\mathbf{v} = \mathbf{l}$ and the small strain rate tensor $\dot{\boldsymbol{\epsilon}}$ are as follows:

$$\bar{\dot{\mathbf{F}}} = \{\dot{\mathbf{F}}\}_{V_m} + \frac{1}{V}\int_{\partial V_c} \dot{\mathbf{b}}\otimes\mathbf{N}\,dS, \tag{2.4}$$

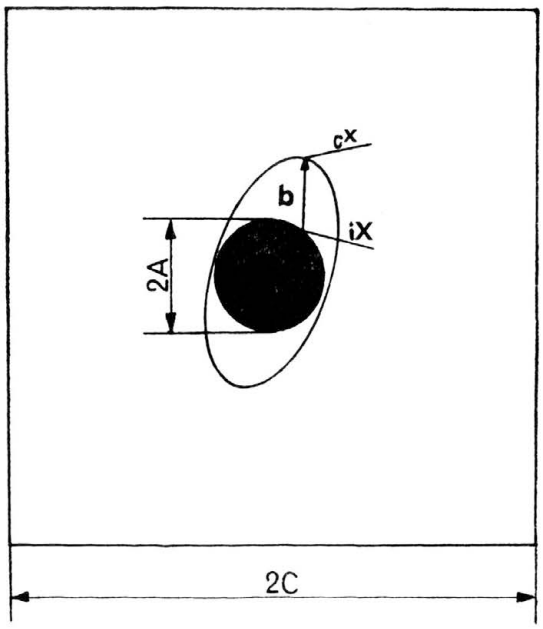

FIG. 1. Basic cell and debonding vector **b**.

$$\bar{\mathbf{l}} = \{\mathbf{l}\}_{v_m} + \frac{1}{v}\int_{\partial v_c} \dot{\mathbf{b}} \otimes \mathbf{n}\, ds, \tag{2.5}$$

$$\bar{\dot{\boldsymbol{\epsilon}}} = \{\boldsymbol{\epsilon}\}_{V_m} + \frac{1}{V}\int_{\partial V_c} (\dot{\mathbf{b}} \otimes \mathbf{N})_{\mathrm{sym}}\, dS, \tag{2.6}$$

with the notation $\{\xi\}_V = \frac{1}{V}\int \xi dV$ and $\{\xi\}_v = \frac{1}{v}\int \xi dv$, where dV is a differential element of volume in the reference configuration Γ_0 and dv its counterpart in the current configuration Γ_t. The subscript m accompanying V and v indicates the matrix volume in the cell. No confusion should be made between the current volume v (denoting also the respective domain) and the velocity vector $\mathbf{v}$ (vector quantity). The bar placed over a symbol designates a macrovariable (an average) in the sense of the proper limit:

$$\bar{\xi}(z) = \{\xi(z; x)\}_{\mathscr{X}} \tag{2.7}$$

where $\mathscr{X}$ represents the basic cell, see [3, 6] for details. We have $V = |\mathscr{X}|_{\Gamma_0} = \mathrm{vol}\ \mathscr{X}_{\Gamma_0}$; $v = |\mathscr{X}|_{\Gamma_t} = \mathrm{vol}\ \mathscr{X}_{\Gamma_t}$, respectively, and $\mathbf{ds} = \mathbf{n}ds$; $\mathbf{dS} = \mathbf{N}dS$ designating the current and reference surface differential elements. The quantities appearing as the last terms on the right-hand side of Eqs. (2.4)–(2.6) characterize the rate of deformation of a damage zone (cavity) in the cell $\mathscr{X}$. They represent, recpectively, the rates of the mixed, Eulerian and infinitesimal damage tensors. Passing to the indicial notation, we have

$$\dot{\Psi}_{iJ} = \frac{1}{V}\int_{\partial V_c} \dot{b}_i N_J\, dS, \quad \Psi_{iJ} = \frac{1}{V}\int_{\partial V_c} b_i N_J\, dS, \tag{2.8}$$

$$\dot{\psi}_{ij} = \frac{1}{v}\int_{\partial v_c} \dot{b}_i n_j ds, \quad \psi_{ij} = \frac{1}{v}\int_{\partial v_c} b_i n_j ds, \tag{2.9}$$

$$\dot{\varphi}_{ij} = \frac{1}{V}\int_{\partial V_c} \dot{b}_i N_j dS, \quad \varphi_{ij} = \frac{1}{V}\int_{\partial V_c} b_i N_j dS. \tag{2.10}$$

In the infinitesimal context (2.6), the formula (2.10), the distinction between N_K and n_k, dS and ds, between capital and small indices, is no more significant as the distinction between the reference and current configurations is neglected. Practically, when exploiting the surface formula (2.10) one will perform the integration over the interface surface supposed to be known rather than over an unknown a priori cavity surface; see, for example [10]. If there were several defects in the cell $\mathscr{X}$, the respective tensors and their rates (2.8)–(2.10) would contain the sum of corresponding integrals. In the formula (2.10) one can identify the damage parameter proposed by VAKULENKO and KACHANOV jr [12]. According to the terminology proposed in the paper [6, 10], we will use the terms "deterioration", "rate of deterioration" for the symmetric parts of $\boldsymbol{\psi}$, $\boldsymbol{\varphi}$; $\dot{\boldsymbol{\psi}}$, $\dot{\boldsymbol{\varphi}}$ respectively, parallelly to the terms "strain", "strain rate" used in the framework of the classical deformation theory.

DRAGON [1] proposed a homogenization procedure to establish the damage evolution law in terms of the damage tensor $\boldsymbol{\varphi}$. It may be generalized to the advanced (finite) damage problem; see [6], in terms of $\boldsymbol{\psi}$ or $\boldsymbol{\Psi}$. To clarify the approach, we will rest tentatively in the infinitesimal context, though the numerical procedure based on the finite element solution discussed in Sect. 4 will concern the components of Ψ_{iJ}. The procedure in question is based on micromechanical data concerning the local velocity field $\mathbf{v}(x) = \dot{\mathbf{u}}$ within the cell $\mathscr{X}$. Such a field constitutes in general a solution of a local boundary value problem for the cell $\mathscr{X}$ with the loading consisting of a given average value of $\bar{\boldsymbol{\sigma}}$ or $\bar{\boldsymbol{\epsilon}}$. This problem should be properly formulated as regards boundary conditions. Without going into details on different possible, we follow the guidelines and assumptions of Sect. 1 and turn to the "well-posed" boundary conditions reflecting the periodic character of the different field on the microscale, viz:

on ∂V $\boldsymbol{\sigma}\cdot\mathbf{n}$ antiperiodic (opposite on opposite sides of ∂V)

$$\dot{\mathbf{u}} = \bar{\dot{\boldsymbol{\epsilon}}}\cdot\mathbf{x} + \dot{\mathbf{u}}^*(x), \tag{2.11}$$

$\dot{\mathbf{u}}^*(x)$ periodic (equal on opposite sides of ∂V).

The local velocity field $\dot{\mathbf{u}}$ belongs to the set of fields generating periodic strain rate. It is split into a linear and a periodic part; the tensor $\bar{\dot{\boldsymbol{\epsilon}}}$ is the macroscopic (average) strain rate associated with $\dot{\mathbf{u}}$. Parallelly, the local strain rate $\dot{\boldsymbol{\epsilon}}(\dot{\mathbf{u}}(x))$ is split into its average and fluctuating terms:

$$\dot{\boldsymbol{\epsilon}}(\dot{\mathbf{u}}) = \bar{\dot{\boldsymbol{\epsilon}}} + \dot{\boldsymbol{\epsilon}}(\dot{\mathbf{u}}^*), \quad \{\dot{\boldsymbol{\epsilon}}(\dot{\mathbf{u}}^*)\}_{\mathscr{X}} = \mathbf{0}. \tag{2.12}$$

To have the complete statement of the problem, one should put together microscopic constitutive laws for constituents (i.e. these for a matrix and inclusion in our case), the local equilibrium equations $\mathrm{div}_x\boldsymbol{\sigma} = 0$, an average given, e.g. $\{\dot{\boldsymbol{\epsilon}}(\dot{\mathbf{u}})\} = \bar{\dot{\boldsymbol{\epsilon}}}$, and join Eq. (2.11). Suppose that one can resolve the problem in question and get

$$\dot{\mathbf{u}} = \mathbf{v}(\boldsymbol{\epsilon}, x, \ldots). \tag{2.13}$$

The connexion of Eq. (2.13) with the damage and/or deterioration rate (2.10) is direct as $\dot{\mathbf{b}}$ itself represents a local velocity vector on the cavity surface (see Eq. $(2.3)_2$)

$$\dot{\mathbf{b}} = {}_c\dot{\mathbf{x}} = \mathbf{v}(\bar{\dot{\boldsymbol{\epsilon}}}, x, \ldots)|_{cx}. \tag{2.14}$$

We may express the position vector ${}_c\mathbf{x}$ on the cavity surface in the form

$${}_c\mathbf{x} = \mathbf{x}^0 + \mathbf{b}, \tag{2.15}$$

where, in comparison with Eq. $(2.3)_1$, we discard $\mathbf{X}$ and put $\mathbf{x}^0$ to indicate infinitesimal damage context. We have now to integrate the tensor product of the type

$$\dot{b}_i(\bar{\dot{\boldsymbol{\epsilon}}}, \mathbf{x}^0 + \mathbf{b}, \ldots)N_j \tag{2.16}$$

over the interface, i.e. inclusion surface having the outer normal $\mathbf{N}(S_c \simeq s_c$ in the infinitesimal context) according to the formula (2.10). This integration standing for a homogenization procedure makes appear integrals involving dyadic expressions $b_i N_j$, i.e. the components of φ_{ij}. We thus arrive at the damage evolution equation having the form

$$\dot{\boldsymbol{\varphi}} = \dot{\boldsymbol{\varphi}}(\bar{\dot{\boldsymbol{\epsilon}}}, \boldsymbol{\varphi}, k), \tag{2.17}$$

where k resulting in particular from the integration for $\mathbf{x}^0$ is a parameter characterizing eventually the inclusion size and spacing, i.e. the type of periodicity under consideration, see [1]. For the sake of simplicity, in Eq. (2.17) and possibly in some other expressions we use the same symbol for a function and its value.

The particular form of Eq. (2.17) obtained from a semi-analytical approximation of the local field (2.13) for a cell composed of an elasto-plastic matrix and a cavity is given in [6]. In the same paper the difficulties of homogenization in the presence of nonlinear constituents (and, in particular, that of elastic-plastic constituents) are briefly resumed, see also SUQUET [3]. In [6] the periodicity of voids distribution was assumed. The elementary cell problem with a cavity in a periodic structure in the context of plasticity was studied frequently using the finite-element method. To the best of the authors knowledge the pioneering work was that of NEEDLEMAN [13]. However, there are no partial results concerning the velocity and/or displacement field that could serve us to construct the evolution equation (2.17). We found it thus propitious to proceed with the following investigation:

(i) experimental tests that might simulate ductile damage by void growth from inclusions and provide us with reasonable void-disturbed local velocity estimations;

(ii) the finite element simulations in an elastic-plastic context aiming to describe the evolution, accounting for the separation and further void growth from an inclusion, and considering different global histories;

(iii) numerical homogenization based on (ii) resulting in global description of damage by cavity growth in terms of damage tensor components.

3. Experimental modelling

DESOYER [8] performed a series of experimental tests aiming to follow the void growth from artificial cylindrical inclusions embedded in an aluminium plate. The double periodic square and hexagonal arrangements of inclusions were realized. The aim was to give access to mechanical factors conditioning void growth, these factors being hardly accessible

on the metallurgical scale level. So, the approach was in the spirit of the macroscopic modelling of damage by LITEWKA and SAWCZUK [14] and CORDEBOIS [15] with the characteristic remark that in Desoyer's investigation the local response within a basic cell was the centre of interest. The laser-speckle measurements of displacement increments were performed within a cell chosen while the whole structure was loaded to the plasticity range with cavity growth occurring. Some preliminary results were presented by DRAGON and DESOYER [16].

Simultaneously with experimental tests and basically local considerations, the finite element analysis was performed for the whole structure (with a limited number of inclusions /cells). Its aim was to evaluate the border effects for a whole specimen, the validity of the Hill macrohomogeneity assumption and the periodicity property for the displacement and deformation fields. The results for the model structure are particularly positive as regards the periodicity of local fields calculated in a series of contiguous cells taken in diverse directions (parallelly to the whole specimen axis, transversally and obliquely).

4. Finite element simulation for the basic cell with inclusion. Numerical results

In connection with the foregoing programme and with the aim to approach in some way the in situ state for a representative volume inside the aggregate with inclusions and/or microcavities we assume the periodicity boundary conditions (2.11) for the unit cell problem. Following [7], this choice is a largely simplified but accessible way to account for the effect of other cavities for the one in the cell under consideration. The double square array is considered. The symmetries resulting from the latter permit to formulate the local problem for a quarter-cell. Its subdivision into finite elements and the types of elements chosen for the plane strain elastic-plastic analysis are given in Fig. 2. They are

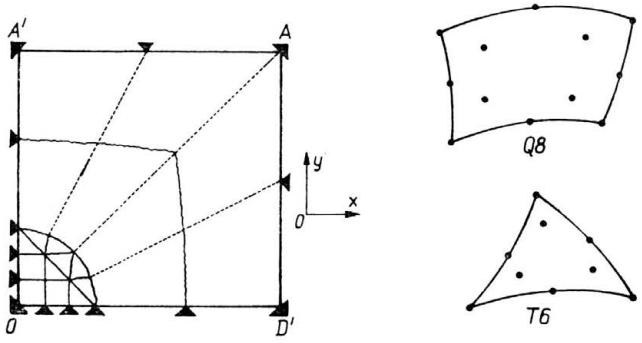

FIG. 2. Elements employed, basic cell mesh and boundary conditions.

the 6-node+3 Hammer integration-point triangular element T6,

the 8-node+4 Gauss-point quadrilateral element Q8.

Both elements admit a quadratic displacement variation. The total number of nodes in the mesh is 73 for 23 elements, namely:

eight T6 elements,

eleven Q8 elements,

four contact elements on the interface inclusion/matrix.

The contact elements are singular layer elements obeying the Coulomb friction rule completed to account for the normal debonding. So, the minimum node separation distance is fixed. Below it the perfect adherence conditions are assumed. In addition to the friction coefficient, the contact element is characterized by its normal (tension-compression) and shear stiffness parameters. The friction coefficient should be chosen rather great to simulate the matrix-inclusion cohesion. Generally the normal (compression) stiffness KN is very high during contact (KN1) to ensure the matter non-penetrability. The same is valid for shear stiffness KS1 when no gliding occurs. On the contrary, when the interface separates, the normal "tensile" stiffness KNO becomes small and the contact element behaves then as a boundary. Much the same is the shearing stiffness variation if gliding occurs. In our case the respective values chosen are as follows:

$$\text{KN1} = \text{KS1} = 10^7 \text{ MPa},$$

$$\text{KNO} = \text{KSO} = 10^{-3} \text{ MPa}.$$

The finite element mesh may seem rather simple to take into account complex stress/strain configurations in the matrix in the vicinity of inclusion/cavity. However, it has been confirmed by other calculations in the plasticity context that multiplication of elements beyond the number mentioned above for a quarter-cell has no significant effect on final results, see, for example, the work of DEBORDES *et al.* [17] on the limit load evaluation for an analogous cell with a hole. The last work cited employed of course the same code MEF (origin UTC Compiegne; G. Touzot) as the present study.

The matrix material is an elastic-plastic isotropically hardening solid. The calculations were carried out using the MEF version employing the large plastic deformation model by SIDOROFF [18] adapted to the code structure by Debordes. The material parameters employed are these of the 1050 A aluminium after annealing (400°C, 1 hour), producing recrystallization and thus increasing the ductility. The elastic moduli are $E = 70$ GPa, $\nu = 0.3$, the uniaxial yield stress $\sigma_Y = 14$ MPa. For computation the hardening curve is introduced point-by-point. The inclusion material is described by the same mechanical model as the matrix material. However, due to elevated elastic stiffness, $E = 210$ GPa, and higher plasticity limit, $\sigma_Y = 500$ MPa for the inclusion compared to the matrix material, no plastic deformation occurred in our analysis carried out for different loading paths up to the global mean strain $\bar{E}_{yy} = 12.5\%$. The symbol $\bar{E}_{ij}$ stands for the global accumulated strain components defined by

$$\bar{E}_{ij} = \int_0^t \bar{d}_{ij}\, dt, \quad \bar{d}_{ij} = {}_{\text{sym}}\bar{l}_{ij} = \bar{v}_{(i,j)}.$$

Numerically, the step-by-step incremental procedure is employed, each step being furthermore discretized into sub-steps. The velocity gradient components $v_{i,j}$ are fairly approximated from displacement increments through the implicit or partially implicit schemes. These variants as well as the integration scheme for the constitutive equation according to the MEF version employed are resumed in [8].

Different global paths are examined. They are characterized by the ratio $\alpha = \bar{E}_{yy}/\bar{E}_{xx}$ indicating the external profile of the unit cell deformed. Each loading path was monitored by imposing the $\Delta\bar{E}_{ij}$ increment for each element through the supplementary fictitious node. Consequently, the displacement and deformation increments effectively calculated in nodes and the Gauss points of finite elements concern uniquely the locally fluctuating part of these quantities (see Eqs. (2.11) and (2.12) by analogy in the infinitesimal context). Practically the $\Delta\bar{E}_{yy}$ increments corresponding to consecutive loading steps were fixed and the relative $\Delta\bar{E}_{xx}$ values were calculated: $\Delta\bar{E}_{xx} = \Delta\bar{E}_{yy}/\alpha$. Eight loading steps were considered for each α. The corresponding $\Delta\bar{E}_{yy}$ increments are as follows:

Step 1: $\Delta\bar{E}_{yy} = 0.05\%$; Step 2: $\Delta\bar{E}_{yy} = 0.5\%$;

Steps 3—6: $\Delta\bar{E}_{yy} = 1\%$; Steps 7—8; $\Delta\bar{E}_{yy} = 4\%$.

Selected results relevant to the loading paths corresponding to $\alpha = \infty$, i.e. $\bar{E}_{xx} = 0$; $\alpha = 1$; $\alpha = 2$; $\alpha = -1.5$ and $\alpha = -3$ are illustrated in Figs. 3–6.

The displacements charts related to the loading paths $\alpha = \infty$ and $\alpha = -1.5$ are shown in Fig. 3. For $\alpha = \infty$ corresponding to unidimensional global deformation and multiaxial

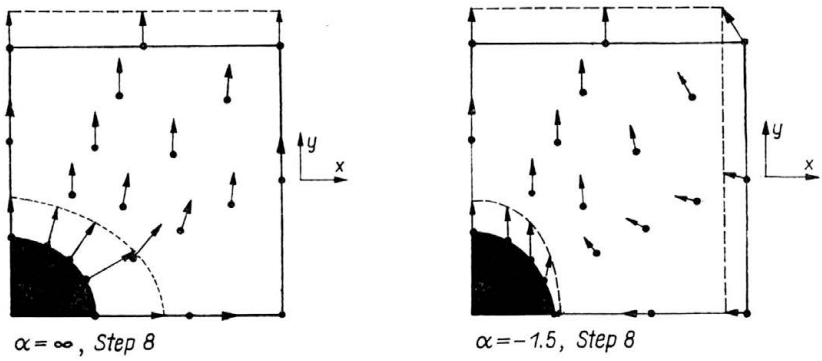

$\alpha = \infty$, Step 8 $\alpha = -1.5$, Step 8

FIG. 3. Cavity form and displacement maps at last step of loading for two values of α.

tensile stress state, an oblate shape of the cavity is observed, i.e. its extension opposed to the global strain aspect. This result is in agreement with the finite element study by NEMAT-NASSER and TAYA [19] of the problem of a unit cell with a hole, i.e. neglecting the inclusion effect. The oblateness effect was studied, for an infinite block of nonlinear viscous solid containing an isolated void, by BUDIANSKY *et al.* [20]. We may note, following the last authors, that this effect is "obviously significant in void interaction and coalescence under tensile straining". The case $\alpha = -1.5$ approaches the in-plane loading path for the basic cell at the experimental investigation summarized in Sect. 3. However, due to the out-of-plane deformations within the cell in experimental procedure, one can admit merely qualitative comparisons of respective results.

Having established the "reactions" $\bar{\sigma}_{ij}$ for macrostrains imposed in each element, we were able to trace the curves shown in Fig. 4 representing the mean global stress components $\bar{\sigma}_{yy}$, $\bar{\sigma}_{xx}$ versus $\bar{E}_{yy}$. The abscissa scale chosen and sometimes the magnitude of $\Delta\bar{E}_{yy}$ for the first step of loading eliminates parts of the mounting branches in some cases.

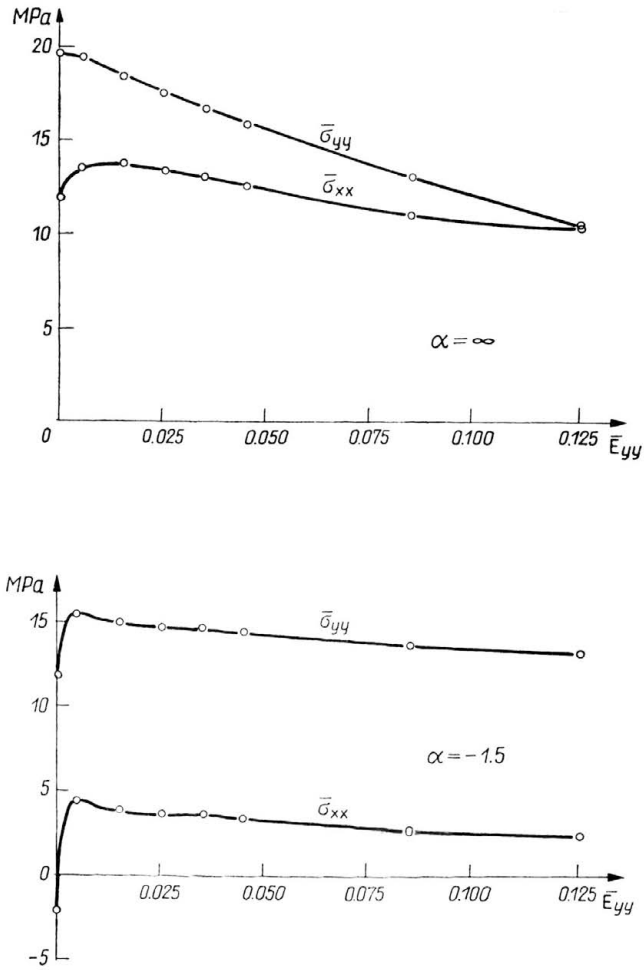

FIG. 4. Macrostress–macrostrain curves for two values of α. Softening effect.

However, the interest lies mainly in exemplifying the descending branches (global softening) due to cavity growth. One may conclude that the inclusion presence influences the curves by provoking a load drop more pronounced in the vicinity of the maximum in comparison to analogous curves for a finite cell with a cylindrical void (hole), even if in the latter context the emerging of secondary voids is simulated by vanishing of elements in the matrix, see LI *et al.* [21]. The stress drop effect may be related to advanced inclusion debonding and depend in general on inclusion size and spacing.

Another effect of inclusion presence is illustrated in Fig. 5 where the effective plastic strain maps are given for $\alpha = -1.5$ respectively for the cell with a hole growing from initial circular cylindrical shape and for the cell with a cavity growing from an inclusion. The strain concentration in the vicinity of the debonding point is clearly perceived in Fig. 5b; note also the cavity form after partial separation. The respective frontiers of the elastic-plastic zone near the horizontal axis are noticeably different.

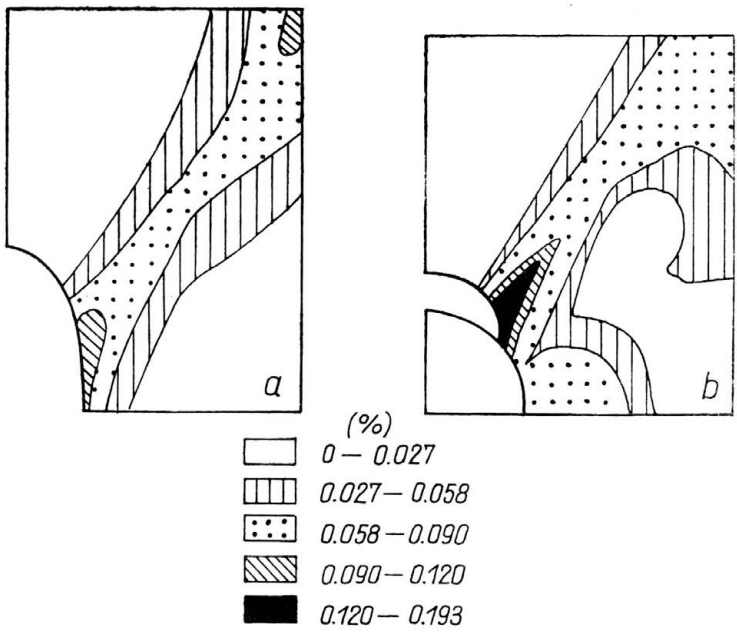

FIG. 5. Maps of equivalent plastic strain after the first step of loading for $\alpha = -1.5$; a) basic cell with a hole, b) basic cell with an inclusion.

The displacements calculated by finite element analysis in the nodes of contact elements give access to the damage tensor components (see Sect. 2). In particular, with respect to the initial interface geometry as the one characterizing the reference configuration, one may compute the components of the mixed (hybrid) damage tensor. It was done using the formula $(2.8)_2$ in a discretized manner, i.e. from the nodal displacement values using the shape functions for contact/border elements. The respective curves giving Ψ_{yy} versus Ψ_{xx} are shown in Fig. 6. We find for $\alpha = 2$ and $\alpha = \infty$ the curves indicating $\Psi_{xx} >$

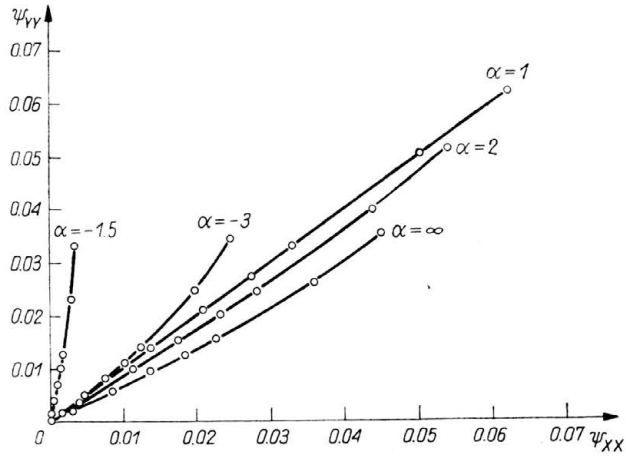

FIG. 6. Damage kinetics; $\Psi_{yy} - \Psi_{xx}$ curves for the five values of α studied.

$> \Psi_{yy}$, i.e. greater global cavity extension along the x-axis while the global straining aspect is inverse: $\bar{E}_{yy} > \bar{E}_{xx} \geqslant 0$. This illustrates again the oblateness effect remarked before.

5. Concluding remarks

The finite element study of the problem of the unit cell in the aggregate composed of an elastic-plastic matrix and cavities formed around periodically set inclusions permitted to evaluate the inclusion effect on the cavity growth and shape, on the concentration of plastic strain in the matrix during inclusion-matrix separation and on the overall stress-strain behaviour for different loading histories. The inclusion-matrix interface was modelled using special contact finite elements capable of accounting for the normal and gliding separation modes corresponding to the one of ductile fracture damage mechanisms. The modelling presented made it possible for the numerical homogenization to give an overall damage-kinetics representation in terms of damage tensor components. It may encourage further studies on the relative phenomena tending to better evaluations of ductily limits of engineering materials.

The results presented agree with the output of the homogenization model relating the damage evolution to actual accumulated damage and to a parameter relative to inclusion size and spacing, i.e. finally to the void nucleation and growth history. Other recent finite element-based analyses (see, for example, [21]), even when neglecting the inclusion effect, conclude with the similar assertion, i.e. stress the effect of void shape and growth history on actual behaviour and ductility limits. It seems that accounting for the nucleation mechanism, i.e. for the inclusion presence, contributes to refinement of the like modelling and of final averaging evaluations.

References

1. A. DRAGON, *Plasticity and ductile fracture damage: study of void growth in metals*, Enging. Fracture Mech., **21**, 4, 875–885, 1985.
2. F. BEREMIN, *Experimental and numerical study of the different stages in ductile rupture: application to crack initiation and stable crack growth*, Proc. IUTAM Symp. on Three-Dimensional Constitutive Relations and Ductile Fracture, Dourdan, France, 2–5 June 1980, ed. by S. NEMAT-Nasser, North-Holland Publ. Comp., 185–205, 1981.
3. P. SUQUET, *Approach by homogenization of some linear and nonlinear problems in solid mechanics*, Proc. Int. Coll. CNRS n 319 on Plastic Behaviour of Anisotropic Solids, Villard-de-Lans, 16–19 June 1981, ed. by J. P. BOEHLER, 77–117, Editions du CNRS, Paris 1985.
4. R. HILL, *The essential structure of constitutive laws for metal composites and polycrystals*, J. Mech. Phys. Solids, **15**, 1, 79–95, 1967.
5. E. SANCHEZ-PALANCIA, *Non-homogeneous media and vibration theory*, Springer-Verlag, Berlin 1980.
6. A. CHICHAB, A. DRAGON, *Tensorial damage evolution and coupled plasticity-damage framework*, Proc. IUTAM Symp. Yielding, Damage and Failure of Anisotropic Solids, Villard-de-Lans, 24–28 August 1987, ed. by J. P. BOEHLER, Mechanical Eng. Publ. Ltd, London [in press].
7. P. GILORMINI, C. LICHT, P. SUQUET, *Growth of voids in a ductile matrix: a review*, Euromech Coll. Postcritical Behaviour and Fracture of Dissipative Materials, Jabłonna, Poland, 1986; Arch. Mech., **40**, 1, 43–80, 1988

8. T. DESOYER, *Etudes numérique et expérimentale de l'évolution de cavités autour d'inclusions en milieu élastoplastique quasi-périodique. Relation avec un modèle d'endommagement ductile.* Doctoral Thesis, University of Poitiers, 1987.
9. H. D. BUI, K. D. VAN, C. STOLZ, *Relations entre les grandeurs macroscopiques et microscopiques pour un solide élastique-fragile ayant des zones endommagées*, C.R. Acad. Sci., Paris, 292, 12, 863–866, 1981.
10. A. DRAGON, A. CHIHAB, *On finite damage: ductile fracture damage evolution*, Mech. Materials, **4**, 1, 95–106, 1985.
11. H. HORII, S. NEMAT-NASSER, *Overall moduli of solids with microcracks: load-induced anisotropy*, J. Mech. Phys. Solids, **31**, 2, 155–171, 1983.
12. A. A. VAKULENKO, M. L. KACHANOV, *Continual theory of a medium with cracks*, Mekhanika Tverdogo Tela (Mechanics of Solids), 6, 159–166, 1971 [in Russian].
13. A. NEEDLEMAN, *Void growth in an elastic-plastic medium*, Trans. ASME, J. Appl. Mech., **39**, 964–970, 1972.
14. A. LITEWKA, A. SAWCZUK, *Experimental evaluation of the overall anisotropic material response at continous damage*, in: Mechanics of Material Behaviour, the D.C. Drucker Anniversary Volume, ed. G. J. DVORAK, R. T. SHIELD, 239–252, Elsevier, Amsterdam 1984.
15. J. L. CORDEBOIS, *Comportements et résistance de milieux métalliques multiperforés*, J. Méc. Appl., **3**, 119–142, 1979.
16. A. DRAGON, T. DESOYER, *Finite and infinitesimal damage; study of evolution and experimental simulation*, Trans. ASME, J. Pressure Vessel Techn., **110**, 4, 348–354, 1988.
17. O. DEBORDES, C. LICHT, J. J. MARIGO, P. MIALON, J. C. MICHEL, P. M. SUQUET, *Charges limites de milieux fortement hétérogènes*, Rapport de fin de Contrat MIR n 83-S-0780, Note Technique 85-3, Université de Montpellier, 1985.
18. F. SIDOROFF, *Incremental constitutive equation for large strain elasto-plasticity*, Int. J. Engng. Sci., **20**, 1, 19–26, 1982.
19. S. NEMAT-NASSER, M. TAYA, *Model studies for ductile fracture*, in: Continuum Model of Discrete Systems, ed. J. W. PROVAN, 387–405, University of Waterloo Press, 1978.
20. B. BUDIANSKY, J. W. HUTCHINSON, S. SLUTSKY, *Void growth and collapse in viscous solids*, in: Mechanics of Solids, the R. Hill 60th Anniversary Volume, ed. H. G. Hopkins, M. J. Sewell, 13–45, Pergamon Press, Oxford 1982.
21. G. C. LI, T. GUENNOUNI, D. FRANÇOIS, *Ductile damage caused by two generations of voids*, CNRS-GRECO Deformations et Endommagement, Res. Rep., 1987.

UNIVERSITE DE POITIERS
LABORATOIRE DE MECANIQUE DES SOLIDES, POITIERS
et
LABORATOIRE DE MECANIQUE ET D'ACOUSTIQUE
MARSEILLE, FRANCE.

Received March 24, 1988.